

Real Time Core Loss Estimation for the Wound Rotor Synchronous Machine

Bernard Steyaert
Columbia University

bernard.steyaert@columbia.edu

Ethan Swint
Tau Motors

ethan@taumotors.com

W. Wesley Pennington
Tau Motors

wesley@taumotors.com

Matthias Preindl
Columbia University

matthias.preindl@columbia.edu

Abstract—Estimation of electrical losses for machines is important to operating them efficiently. Although copper loss is typically the dominant form of electrical losses in an electric machine, core loss also contributes significantly especially at high speed. In this study, two simple analytical model for core loss are proposed for the wound rotor synchronous machine using the least squares method and validated through FEA simulation. The proposed core loss estimation methods have 12% and 53% average error over all operating points of the machine. They are extremely light computationally and use very few coefficients making them viable options for real-time controllers for various applications.

Index Terms—Loss Minimization, Motor Parameters, Core Loss, Wound Rotor Synchronous Machine

I. INTRODUCTION

Reference generation maps for electric machines take some combination of torque and (sometimes) speed and output a set of currents that minimizes the electrical losses of the machine. The dominant losses are copper loss and core loss, which are generally proportional to torque and speed, respectively.

Selecting the most optimal (efficient) reference current given a speed and torque requires an accurate representation of these losses over the full operating range of currents the machine is rated for. In the most generalized sense, an attempt to differentiate these losses by relating them to a quantity proportional to the product of speed and torque, each to an arbitrary power, can be made and is very effective [1]. Mapping these references to a useful format for a microcontroller (MCU) to use in real-time such as a look up table (LUT) or piecewise affine (PWA) map is a separate and interesting challenge [2], [3].

These maps are complex, not easily built, and are designed specifically to create offline efficiency maps to load and run on a microcontroller, such as MTPA. They also require a large dataset of the machine speed, torque, current, copper loss, and core loss, which may not always be available to machine control engineers. These are typically obtained through FEA and/or experimentation.

Machine design engineers design machines to minimize core loss by analyzing the effects of eddy currents, hysteresis, and armature reaction effects with different geometries, materials, and laminations [4]–[7]. For the wound

rotor synchronous machine (WRSM) this is especially important as its primary application until recently has been MVA-sized machines for power generation. In these applications, the electrical speed is fixed, and the core losses can be optimized for this specific speed.

The WRSM has seen a recent increase in popularity in automotive applications, as it is a compromise to the high power density (efficient and expensive) Permanent Magnet Synchronous Machine (PMSM) and low power density (inefficient and cheap) Induction Machine (IM), which are the two most popular machines in space [8], [9]. An interesting development in WRSMs is the use of hairpin windings to increase slot fill factor [10], but increases core losses and introduces additional manufacturing complexity [11]. Automotive applications for machines require efficient use for a wide range of speeds and torques, requiring a revisit to core and copper loss models for the machine. For this reason, it is not enough to simply design WRSMs to minimize copper loss, but for core loss as well. This has already been studied and combined with MTPA (maximum torque per ampere) for the PMSM machine in a so-called Maximum Efficiency per Ampere (MOPA) [12] among other names, however the work is unvisited for the WRSM.

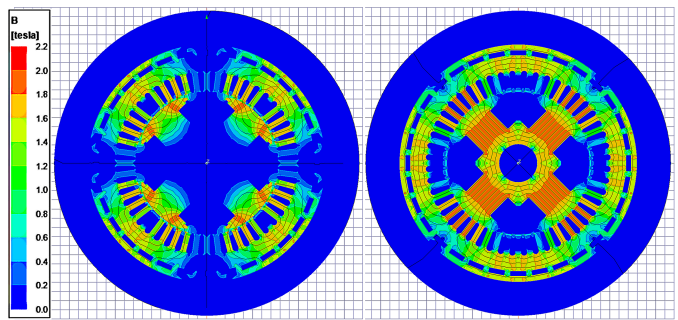


Fig. 1: WRSM cross section showing a saturated flux density B distribution in Tesla at $i_q = 1(\text{pu})$ (left), and $i_d = 1(\text{pu})$ (right)

An understanding of core losses with a simple model (in addition to copper losses) can be used to predict the temperature of the machine, especially at high speeds when core loss is most significant. Power dense wound field machines, especially those with brushes, must have their temperature maintained to avoid mechanical failure.

Furthermore, an increase in temperature in the machine increases its thermal resistance, which decreases efficiency and leads to even more temperature increase. The ability to accurately and quickly predict thermal losses can more quickly inform cooling measures to begin, whether air or liquid [13], [14].

In this study, two simple core loss models are proposed which utilize the least squares method for determining a quadratic core loss function. The core loss is proportional to the square of the machine speed and square of the machine flux. The proposed models have 12% and 53% average error when compared to FEA. The models require only 9 or 729 coefficients each. Proposed use-cases of the models are maximum efficiency point selection, use in real-time control, and FEA outlier detection.

The paper is organized as follows, the basic machine model is introduced in Section II, core loss modelling is discussed in Section III, results for a 65 kW machine are shown in Section IV, analysis of the results against an FEA map are in Section V, and the paper is concluded in Section VI.

II. MACHINE OPERATION

The current in a three-phase WRSM has two parts, the AC stator current i_{dq} which utilizes the dq-axis from the power-invariant Clarke-Park transform, and DC rotor (sometimes called field) current i_r . The rotor is aligned to the stator d-axis. These are combined into the column vector $i_{rdq} = [i_r \ i_d \ i_q]^T \in \mathbb{R}^3$.

The relationship between the current $i_{rdq} \in \mathbb{R}^3$ and flux of the machine $\lambda_{rdq} \in \mathbb{R}^3$ is non-linear, and has saturation and cross saturation effects. This can be modelled by the continuous nonlinear function, and the flux distribution at full current is shown in Fig. 1.

$$\lambda_r = f_r(i_r, i_d, i_q), \quad (1a)$$

$$\lambda_d = f_d(i_r, i_d, i_q), \quad (1b)$$

$$\lambda_q = f_q(i_r, i_d, i_q), \quad (1c)$$

The dq-axis stator current of the machine is limited by a stator rated current $i_{s,r}$, while the rotor axis current is limited by a rated rotor current $i_{r,r}$. These limits are typically set by thermal constraints. The current set \mathcal{I} is thus constrained by a cylindrical shape.

By (1) the flux set is constrained to

$$\lambda \in \Lambda = \{\lambda_{rdq} \in \mathbb{R}^3 \mid g \circ \Lambda = \mathcal{I}\}. \quad (2)$$

where $g(\lambda) = i$ is the inverse function of (1).

The torque per pole pair of the machine is defined by $\tau_p(i, \lambda) : \mathbb{R}^6 \rightarrow \mathbb{R}$

$$\tau_p(i, \lambda) = i^T \mathbf{J} \lambda, \quad (3)$$

where \mathbf{J} is the stator cross product matrix

$$\mathbf{J} = \begin{bmatrix} 0 & 0 & 0 \\ 0 & 0 & -1 \\ 0 & 1 & 0 \end{bmatrix} \quad (4)$$

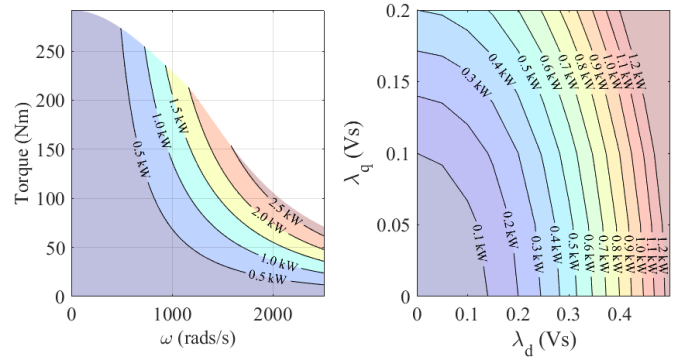


Fig. 2: $\pi_{fe, glo}$ (Left) core loss vs torque and speed, (Right) core loss vs stator flux (fixed speed)

and $p \in \mathbb{R}$ is the number of pole pairs of the machine.

The maximum torque T_{max} and speed ω_{max} are generally limited by mechanical constraints. The rotor and stator can be “flux weakened” in the sense of a PMSM such that electrically there is one maximum torque (at $i_{r,r}$ and $i_{s,r}$) and a theoretically unlimited electrical speed.

III. CORE LOSS MODELS

The most general and possibly most common core loss (often times referred to as iron loss, or π_{fe}) model is the Steinmetz Equation, which in its simplest form is

$$\pi_{fe} = k f_s^a B_m^b \quad (5)$$

where k is a coefficient, f_s is the switching frequency, B_m is the peak value of the magnetic flux density. For machines, the machine speed is the rate at which the magnetic flux of the core material changes, so ω replaces f_s . Flux density B_m is proportional to the more commonly used machine flux λ which leads to the equation

$$\pi_{fe} = k \omega^a \lambda^b. \quad (6)$$

This equation is too general to apply to a real-world system, the choice of discrete exponents a and b for a given number of terms is done to best fit magnetic flux and frequency to the core loss of the system being tested. There are many variations of (6) used in motor loss modelling, but one called the Bertotti iron loss formula [12] uses terms representing hysteric loss, lamination thickness, and excess loss with coefficients (a, b) of $(2, 1)$, $(2, 2)$, $(1.5, 1.5)$ as

$$\pi_{fe} = k_h \omega \lambda^2 + k_d^2 \omega^2 \lambda^2 + k_e \omega^{1.5} \lambda^{1.5}. \quad (7)$$

The relationship between terms in (6) and coefficients (a, b) is an open research question [15]. This equation is problematic for machines that have coupled flux, as it is nontrivial compute non-integer matrix exponents.

We propose two core loss models which are very simple. The first is

$$\pi_{fe} = k \omega^2 \lambda^2, \quad (8)$$

which if we consider λ is a $[3 \times 1]$ matrix from (2) becomes

$$\pi_{fe, glo} = \omega^2 \lambda^T \mathbf{G} \lambda \quad (9)$$

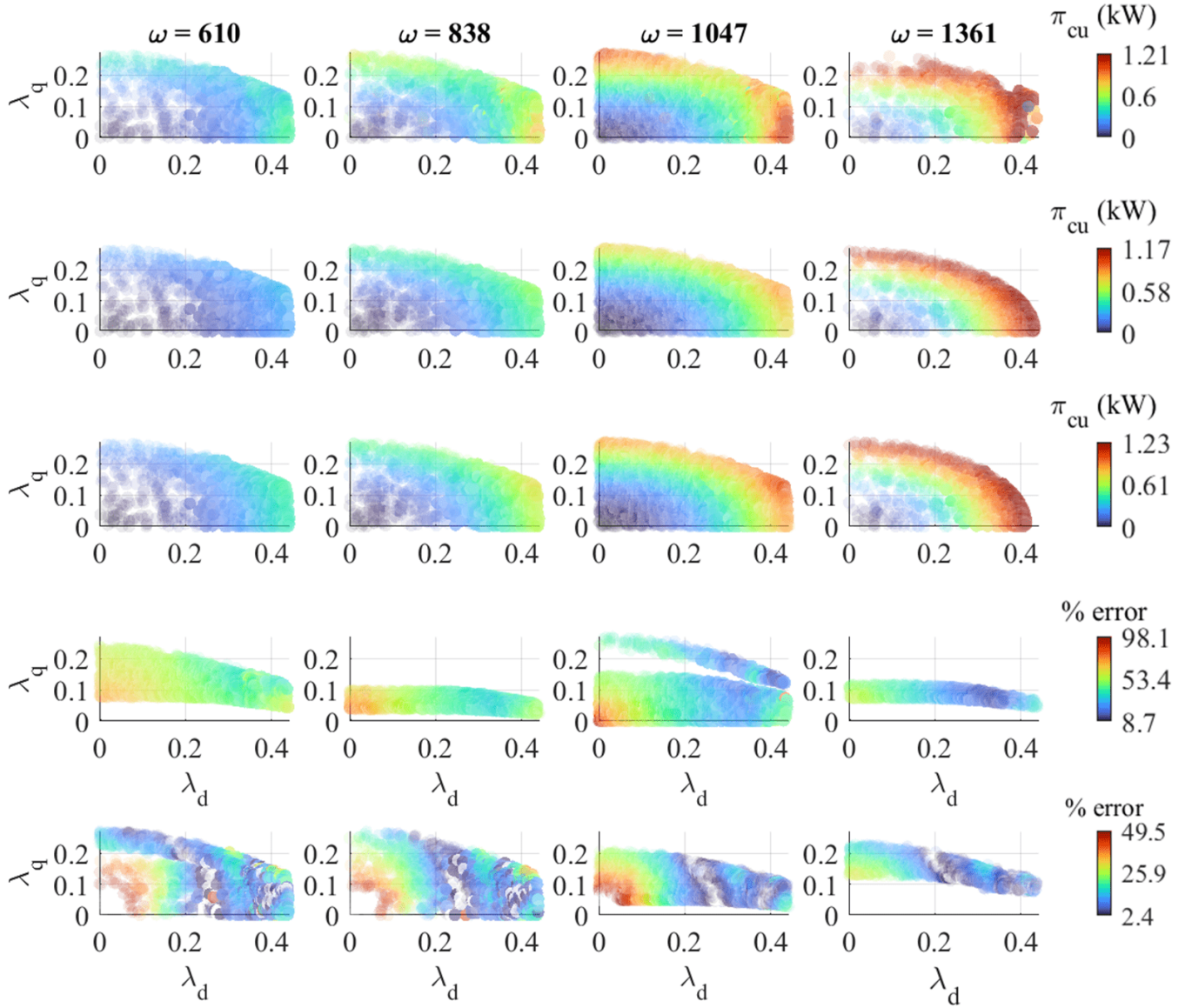


Fig. 3: (first row) π_{fe} FEA, (second row) $\pi_{fe,glo}$, (third row) $\pi_{fe,bin}$, (fourth row) error between π_{fe} and $\pi_{fe,glo}$, (fifth row) error between π_{fe} and $\pi_{fe,bin}$

where the coefficient k is distributed into the matrix \mathbf{G} . Because the exponent $a = 2$, the squared term of flux λ is simple to compute. A linear term $a = 1$ could potentially be added. This model can be called the global model, or $\pi_{fe,glo}$. Torque and speed both contribute to this π_{fe} equation, speed proportional to the ω^2 term and torque by the flux term λ in (3). The trend of the model against torque, speed, and flux is shown in Fig. 2.

The second model is

$$\pi_{fe,bin} = \begin{cases} \omega^2 \lambda^T \mathbf{G}_{q,1} \lambda + \omega \lambda^T \mathbf{G}_{l,1} \lambda + \lambda^T \mathbf{G}_{o,1} \lambda & \omega \in \Omega_1 \\ \omega^2 \lambda^T \mathbf{G}_{q,2} \lambda + \omega \lambda^T \mathbf{G}_{l,2} \lambda + \lambda^T \mathbf{G}_{o,2} \lambda & \omega \in \Omega_2 \\ \vdots & \\ \omega^2 \lambda^T \mathbf{G}_{q,n} \lambda + \omega \lambda^T \mathbf{G}_{l,n} \lambda + \lambda^T \mathbf{G}_{o,n} \lambda & \omega \in \Omega_n \end{cases} \quad (10)$$

where the Ω_j is a subset of electrical speeds of the machine, $\Omega_j = \{\omega \in \mathbb{R} \mid \omega_{j,\min} < \omega_j \leq \omega_{j,\max}\}$. The speeds of the machine can be evenly or unevenly distributed into n subsets which cover all machine speeds $\Omega = \{\Omega_1 \cup \Omega_2 \cup \dots \cup \Omega_n\}$. The model (10) has n piecewise quadratic equations which each have three matrices of coefficients corresponding to the quadratic dependence on speed (\mathbf{G}_q), linear dependence on speed (\mathbf{G}_l), and no dependence on speed (\mathbf{G}_o), and can be formulated to be continuous. This core loss model is binned by speed, and thus denoted $\pi_{fe,bin}$.

For the global model (9) the matrix \mathbf{G} is obtained by first having a set of available loss datapoints $\{\pi_{fe}, \lambda, \omega\}$ and solving the following convex optimization problem using

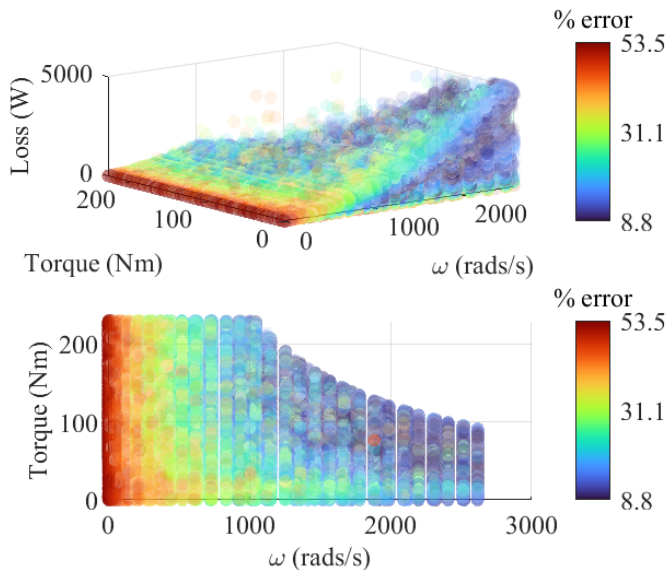


Fig. 4: Core loss vs speed and torque, color is core loss error vs FEA, $\pi_{fe, glo}$

all points

$$\text{minimize } \|\omega^2 \lambda^T \mathbf{G} \lambda - \pi_{fe}\| \quad (11a)$$

$$\text{subj. to } \mathbf{G}_{(i,j)} \geq 0, \quad (11b)$$

where \mathbf{G} is the optimization variable. The only constraint is that that coefficients must all be non-negative. This is the least squares solution for overdetermined systems. The optimization is run over all datapoints (many speeds) to obtain an “averaged” \mathbf{G} which best fits the loss to all data. The components of \mathbf{G} along the diagonal, i.e. $\mathbf{G}_{(1,1)}$, $\mathbf{G}_{(2,2)}$, $\mathbf{G}_{(3,3)}$ model the self-induced core loss, i.e. $\mathbf{G}_{(3,3)}$ quantifies how much loss is contributed from the q-axis flux λ_q^2 . In many cases the rotor is excited with a DC current, which produces a constant flux λ_r , in which case the core loss from just λ_r^2 will be very small, and $\mathbf{G}_{(1,1)}$ will be negligible. Non-diagonal terms represent losses induced from flux-coupling between different axis.

For the second model, the $\mathbf{G}_{q,j}$, $\mathbf{G}_{l,j}$, and $\mathbf{G}_{o,j}$ matrix coefficients are computed per speed ω_j by

$$\text{minimize } \|\omega^2 \lambda^T \mathbf{G}_{q,j} \lambda + \omega \lambda^T \mathbf{G}_{l,j} \lambda + \lambda^T \mathbf{G}_{o,j} \lambda - \pi_{fe}\| \quad (12a)$$

$$\text{subj. to } \mathbf{G}_{q,j,(i,k)} \geq 0 \quad (12b)$$

$$\mathbf{G}_{l,j,(i,k)} \geq 0 \quad (12c)$$

$$\mathbf{G}_{o,j,(i,k)} \geq 0 \quad (12d)$$

$$\omega \in \Omega_j. \quad (12e)$$

In this model the speed is explicitly set to range specified in (12e), which makes each coefficient matrix speed-independent. Additional constraints can be added to ensure continuity. The optimization problems (11) and (12) can be solved offline to build the core loss models (9) and (10) respectively, which can then be loaded onto a microcontroller for real-time core loss evaluation.

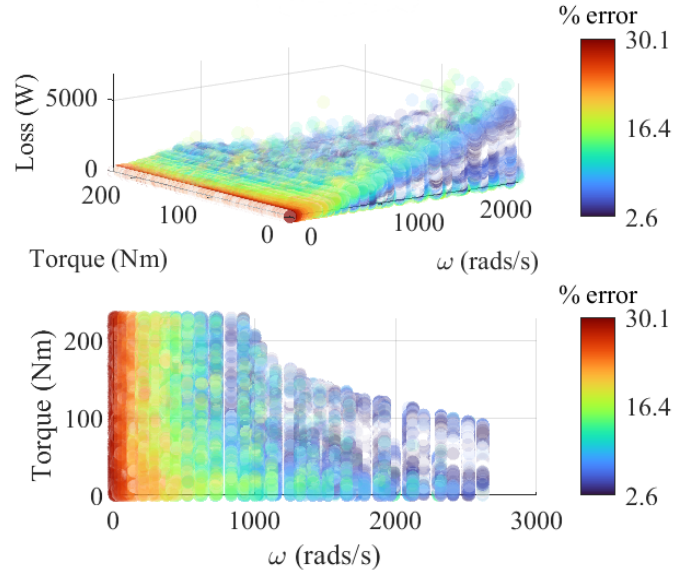


Fig. 5: Core loss vs speed and torque, color is core loss error vs FEA, $\pi_{fe, bin}$

IV. RESULTS

The two core loss models proposed in Section III were run on a 65 kW WRSM with parameters shown in TABLE I. The FEA dataset used had 498,606 FEA datapoints $\{\pi_{fe}, \lambda, \omega\}$ corresponding to the full current range of the machine $i_{rdq} \in \mathcal{I}$ and 81 specific speeds ω_j , each speed corresponds to one speed range Ω_j , so there are $n = 81$ piecewise equations to (10). The values for \mathbf{G} were relatively small for all terms except $\mathbf{G}_{(2,2)}$ and $\mathbf{G}_{(3,3)}$ which are the self-induced stator core losses of the d-axis and q-axis respectively. This is because for this specific WRSM, the rotor is excited by DC current. The output losses from both functions are shown in the flux domain in Fig. 3. The quadratic relationship between core loss and flux is apparent by the circular loss rings of the stator core loss. The quadratic relationship between speed and core loss is also apparent by the increasing losses per speed (columns left to right).

TABLE I: WRSM Motor Drive Parameters

Parameter	Value
Turns ratio N_f/N_s	39
Pole pairs p	2
Stator resistance R_s	11.732 mΩ
Rotor resistance (stator referred) R_r	5.461 mΩ
Shaft inertia	22.76E-3 kg m ²
Nameplate r-axis inductance L_r	1.956 mH
Nameplate d-axis inductance L_d	2.420 mH
Nameplate q-axis inductance L_q	0.789 mH
Base speed	3000 1/min
Max speed	12000 1/min
DC-link voltage	325 V
Maximum power	65 kW
Maximum torque	220 Nm

V. ANALYSIS

Core loss error for the analytical methods and the FEA is shown in torque-speed domain in Fig. 4 and Fig. 5, and in stator flux domain in Fig. 3. Plots showing the error of both core loss models averaged by speed are shown in Fig. 6 and by flux in Fig. 3. The error used is the 2-norm error, which is calculated as

$$\text{error} = \frac{\|\pi_{fe,analy} - \pi_{fe,FEA}\|_2}{\|\pi_{fe,FEA}\|_2}, \quad (13)$$

at low speed the analytical loss is ≈ 0 so the error appears to be 100%. The error tends to decrease dramatically for both models as speed is increased. The average error for $\pi_{fe,bin}$ is 12% compared to an average error of 53% for $\pi_{fe,glo}$. The error tends to be very high at very low speeds, which are infrequent operational areas in most drive cycles.

Each \mathbf{G} matrix has nine coefficients ($[3 \times 3]$). So although the binned method has much lower error, by (10) it has considerably more coefficients to store. Furthermore there will be some computation time to determine which of the piecewise equations to use. For these reasons, $\pi_{fe,bin}$ is much more accurate, but considerably slower than $\pi_{fe,glo}$ on a microcontroller. Reducing terms is an interesting problem and an active area of research.

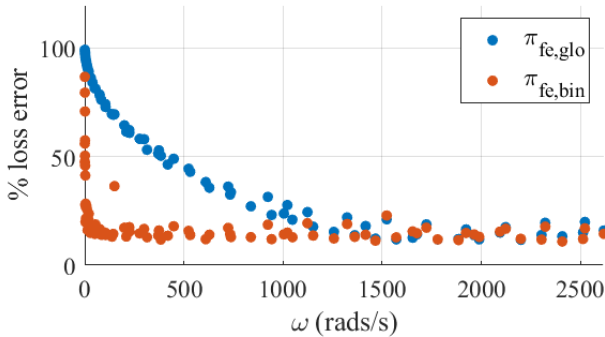


Fig. 6: Average core loss error between FEA and analytical models by speed

The benefits of these two core loss models versus more complex models are 1) Speed of computation 2) Relatively low error 3) No need to know complex machine geometry and 4) Cross coupling core loss is captured. These benefits allow for a wide range of potential applications including fast maximum efficiency point selection, use a cost in a real-time controller when moving between reference speed-torques, and FEA outlier detection.

VI. CONCLUSION

In this study two core loss models are proposed for the WRSM. They are validated using an FEA simulation of the machine, having error of 53% (global) and 12% (binned by speed) respectively. These two core loss models are simple to compute, computationally light, allow

for flux coupling, and can be used for several real-time applications. Topics of further study include: reduction of coefficients, integration into a controller, and pareto-mapping to a reference generation map.

REFERENCES

- [1] A. Mahmoudi, W. L. Soong, G. Pellegrino, and E. Armando, "Loss function modeling of efficiency maps of electrical machines," *IEEE Transactions on Industry Applications*, vol. 53, no. 5, pp. 4221–4231, 2017.
- [2] H. Sano, K. Semba, Y. Suzuki, and T. Yamada, "Investigation in the accuracy of fea based efficiency maps for pmsm traction machines," in *2022 International Conference on Electrical Machines (ICEM)*, pp. 2061–2066, 2022.
- [3] B. Steyaert, E. Swint, W. W. Pennington, and M. Preindl, "Piecewise affine maximum torque per ampere for the wound rotor synchronous machine," in *2022 IEEE Transportation Electrification Conference and Expo (ITEC)*, pp. 356–363, 2022.
- [4] A. Hemeida, P. Sergeant, and H. Vansompel, "Comparison of methods for permanent magnet eddy-current loss computations with and without reaction field considerations in axial flux pmsm," *IEEE Transactions on Magnetics*, vol. 51, no. 9, pp. 1–11, 2015.
- [5] K. S. Garner and M. J. Kamper, "Rotor yoke effect on core losses of a non-overlap wound-rotor synchronous machine," in *2020 International Conference on Electrical Machines (ICEM)*, vol. 1, pp. 2644–2650, 2020.
- [6] M. Biasion, D. Kowal, R. R. Moghaddam, and M. Pastorelli, "Influence of the lamination material and rotor pole geometry on the performance of wound field synchronous machines," in *2022 IEEE Energy Conversion Congress and Exposition (ECCE)*, pp. 1–8, 2022.
- [7] P. Rasilo, A. Belahcen, and A. Arkkio, "Importance of iron-loss modeling in simulation of wound-field synchronous machines," *IEEE Transactions on Magnetics*, vol. 48, no. 9, pp. 2495–2504, 2012.
- [8] D. G. Dorrell, "Are wound-rotor synchronous motors suitable for use in high efficiency torque-dense automotive drives?" in *IECON 2012 - 38th Annual Conference on IEEE Industrial Electronics Society*, pp. 4880–4885, 2012.
- [9] J. de Santiago, H. Bernhoff, B. Ekegard, S. Eriksson, S. Ferhatovic, R. Waters, and M. Leijon, "Electrical Motor Drivelines in Commercial All-Electric Vehicles: A Review," *IEEE Trans. Veh. Technol.*, vol. 61, no. 2, pp. 475–484, Feb. 2012.
- [10] D. B. Pinhal and D. Gerling, "Driving cycle simulation of wound-rotor synchronous machine with hairpin windings considering ac-losses," in *2019 IEEE Transportation Electrification Conference and Expo (ITEC)*, pp. 1–7, 2019.
- [11] M. Kohler, M. Gerngro, and C. Endisch, "A test bench concept and method for image-based modeling of geometric wire bending behavior in needle winding processes," in *2022 IEEE 31st International Symposium on Industrial Electronics (ISIE)*, pp. 1113–1120, 2022.
- [12] R. Ni, D. Xu, G. Wang, L. Ding, G. Zhang, and L. Qu, "Maximum efficiency per ampere control of permanent-magnet synchronous machines," *IEEE Transactions on Industrial Electronics*, vol. 62, no. 4, pp. 2135–2143, 2015.
- [13] D. Fodorean, I.-A. Viorel, A. Djerdir, and A. Miraoui, "Mechanical and thermal designing aspects for a pm synchronous machine with wound rotor," in *2007 International Aegean Conference on Electrical Machines and Power Electronics*, pp. 502–506, 2007.
- [14] J. Godbehere, A. Hopkins, and X. Yuan, "Design and thermal analysis of a rotating transformer," in *2019 IEEE International Electric Machines and Drives Conference (IEMDC)*, pp. 2144–2151, 2019.
- [15] M. C. Kulan, N. J. Baker, K. A. Liogas, O. Davis, J. Taylor, and A. M. Korsunsky, "Empirical implementation of the steinmetz equation to compute eddy current loss in soft magnetic composites," *IEEE Access*, vol. 10, pp. 14610–14623, 2022.